Wiese, B., Nützmann, G. (2011): Calibration of spatial aquitard distribution using hydraulic head changes and regularisation. - Journal of Hydrology, 408, 1-2, 54-66

DOI: 10.1016/j.jhydrol.2011.07.015

Calibration of spatial aquitard distribution using hydraulic head changes and regularisation

Bernd Wiese[1,*] and Gunnar Nützmann[2]
[1] Helmholtz Centre Potsdam, GFZ German Research Centre for Geosciences, Telegrafenberg, D-14473 Potsdam, Germany
[2] Leibniz-Institute of Freshwater Ecology and Inland Fisheries, Müggelseedamm 310, D-12587 Berlin, Germany

Abstract
Irregularly expressed aquitards have a significant impact on hydraulics and redox conditions. The method expands the scope and applicability of characterising spatial structures close to well fields. The test site is an aquifer system with two aquifers divided by an aquitard (glacial till), located at a well field for drinking water abstraction. During operation, the wells are frequently switched and hydraulic head data are recorded at 10 wells in both aquifers. The data contain information about the impact of each abstraction well on each observation well. We develop an inverse modelling procedure to calibrate spatial aquifer parameters from this data. Instead of heads we calibrate to selected head differences to keep the model concise to short term fluctuations and to reduce data. The calibrated model parameters are storativity of the upper aquifer, hydraulic conductivity of both aquifers and leakage of the aquitard. The calibration is carried out spatially by pilot points with the software PEST using regularisation. Different cross validations show that the leakage can be calibrated in a physically meaningful way, but not the hydraulic conductivities and not the storativity. Geostatistic assumptions are not required. The calibrated spatial aquitard distribution coincides with bore profiles and explains anomalies of redox conditions.

Keywords: Inverse modelling, PEST, pilot points, regularisation, aquitard, hydraulic heads, differences, waterworks, pumping test, redox anomaly

* Corresponding author: Helmholtz Centre Potsdam, GFZ German Research Centre for Geosciences, Telegrafenberg, D-14473 Potsdam, Germany, Phone: +49 (0) 331 /288-1823, Fax: +49 (0) 331 /288-1529, mail: wiese@gfz-potsdam.de

1. Introduction

Drinking water often is abstracted from aquifer systems consisting of more than one groundwater story with the aquitards between the stories usually having a strong impact on flow conditions. Though they may be spatially very close together, from conceptual geologic models the flow areas above and below the aquitard are often assumed to be hydrologically well divided. But the dividing layer may have windows where water can penetrate from one aquifer to another. Due to their limited area, streamlines concentrate in these windows, resulting in complex flow fields, which seriously affect the groundwater quality in the managed aquifer system due to the mixing of water from different layers. The detection and location of such aquitard windows however is not trivial. Boreholes only provide information valid for a few square centimeters. Even tiny layers can affect the flow field but the probability of finding it decreases with the drilling diameter, e.g. for production wells. Tracer tests are expensive, may take a long time and often are not allowed if drinking water is abstracted. Geophysical methods may be an alternative, however they also are expensive, and have restricted applicability.

In an earlier study Krabbenhoft and Anderson (1986) demonstrated that ambiguous field data indicate the presence of unexpected factors that may have a marked effect on a subsurface hydrologic system. They prefer the use of groundwater models to isolate the factors that account for an anomalous flow field distribution and related hydraulic gradients in the case of a groundwater/lake system. The importance of the geologic structure for understanding a complex aquifer system is demonstrated in the paper of Martin and Frind (1998), postulating that flow is not so much controlled by the hydraulic conductivity of the different geological units but by their continuity and interconnectivity, particularly in the vertical direction. Their results illustrate the importance of aquitard windows having a controlling influence on flow field distribution. The development of detailed three-dimensional capture zone models for the local well fields with calibration/validation against environmental tracer data was proposed as key techniques to improve the knowledge of the aquifer system. Timms (2001) investigated groundwater quality changes in an aquifer-aquitard system, where near-surface saline water is percolating into a deeper aquifer due to aquitard windows. Inverse mass balance models and an axisymmetric radial groundwater flow model are determined using FEFLOW (Diersch, 1998), furthermore hydrochemical changes were accounted for with PHREEQC (Parkhurst and Apello, 1999). Machado et al. (2007) studied an aquifer-aquitard system in order to understand whether rainfall waters could percolate an upper limestone aquitard and contribute to groundwater storage in the underlying aquifer. In this study they used the groundwater model MODFLOW (Harbaugh et al., 2000) for regional flow modeling and PHREEQC for hydrogeochemical inversion for identifying the contribution of groundwater flow through the Santana aquitard (of unknown hydraulic conductivity) to Cariri Valley aquifers. In a study of Gedeon et al. (2007) regional groundwater flow in NE Belgium was simulated considering two principal types of groundwater circulation. The shallow groundwater circulation is controlled by surface hydrology features. These features influence the groundwater flow in the second aquifer down to a clayey aquitard. In the south of the area, the recharge from the overlying upper aquifer is facilitated by the absence of clay in a limited area, where it has been eroded after sedimentation.

In the present study we investigate groundwater flow in a bank filtration site at the eastern bank of Lake Tegel, Berlin, Germany (Fig. 1). Surface water infiltrates into the groundwater and is abstracted by a well field about 100 m from the lake. The site forms part of Berlin's largest waterworks, affecting an area of 50 km^2. The two existing aquifers are divided by an irregularly formed aquitard consisting of low permeable glacial till. Water infiltrates from the lake into the near surface aquifer. Abstraction wells in the second aquifer cause a downward gradient of hydraulic heads, leading to a downward water flow where the till is nonexistent. A transect of observation wells aligned parallel to the general flow direction provides data about

the hydraulic and geochemical situation. But only a few boreholes exist which show whether the till is existent or not. The picture which they provide about the shape of the till is rough and strongly non-unique and does not fit to hydraulic and geochemical observations. However, a lot of hydraulic information is available. Short term hydraulics at the transect are affected by 7 abstraction wells and recorded by 10 observation wells. A method is developed which allows a spatial aquitard characterisation using operational data and hydraulic heads.

Rötting et al. (2006) carried out inversion of cross hole pumping tests to determine simultaneously aquifer parameters and the hydraulic connection to an adjacent river. We propose an alternative approach of characterising the aquifer properties by using operational data from well fields instead of data from defined tests. By recording the signal of multiple wells in multiple observation wells a large amount of data may be easily collected but the uncertainty has to be estimated because the interval of the recoded data is in the same time scale as the simulated processes. Since the initial water level is not in equilibrium and the geometry usually is complex, traditional pumping test evaluations are not applicable. Numerical simulation is necessary but calibration parameters are strongly cross correlated and simulation results have to be compared and calibrated to a large amount of data. Under these circumstances a thorough calibration can not be performed manually and inverse modeling becomes necessary. The detection of spatial structures which are not known in advance requires a spatial discretisation with numerous parameters. The solution is often not unique and a subset of parameters turns out to be sensitive. The inverse modeling tool PEST (Doherty, 2004) is suitable to solve this problem by constraining a large amount of parameters using regularisation and offering the possibility of performing the inversion within a reasonable time using coarse grain parallel computing.

The probably most important contribution of this study is that subsurface structures are directly deduced from hydraulic data, i.e. the calibrated structure has a pronounced deterministic part that is demonstrated not to be affected by uncertainty. Except for a smoothing constraint, that effectively provides the lower spatial resolution, no assumptions about the aquifer structure are required.

Applied inverse methods demonstrate well matching of observation data and prove predictive capability with respect to observation data. We provide a more rigorous approach and demonstrate that the principal model results are not compromised by model or data inherent uncertainty. The method shows that the conductivity of the glacial till is unique with regard to different subsamples and also to aquifer hydraulic conductivity.

While prediction uncertainty is frequently estimated by resampling in surface water hydrology (Dingman, 2008), we have not found this applied to groundwater. Feyen and Caers (2006) applied resampling to synthetic data. We only found that uncertainty analyses for field data have been carried out by using the complete data set (e.g. Datta et al., 2009, Alcolea et al. 2009). Furthermore, the calibration results are prerequisite for a consistent geochemical interpretation. It has not been reported previously that a geochemical regime can be explained by means of a hydraulic calibration.

The main steps of the procedure are: (1) Based on an existing regional flow model (Wiese and Nützmann, 2009) the actual domain is extracted as a sub-domain of this model and telescoping mesh refinement (Leake and Claar, 1999) is used to set up a telescope model. This minimises the computational time, an important issue for highly parameterised models. (2) Deviations between observed and hydraulic heads in the regional model are between -0.5 m and 0.5 m, but short term head changes due to well operation are less than 0.5 m. The deviations which are caused by inaccuracies from the regional model must not be calibrated within the telescope model. We recalculate hydraulic heads to secondary observations which represent the shape of the short term head variations. This orthogonalises out structural noise and keeps calibration concise to local properties. (2a) The measurement interval of observations and operational data have a frequency and therefore an accuracy of 1 hour,

which is as well the same order of time scale as the hydraulic processes. The model discretisation is adapted to avoid a systematic error due to data accuracy and the remaining uncertainty is estimated. (3) Leakage, unconfined storage coefficient and hydraulic conductivity of both aquifers are parameterised using a grid of pilot points, coarser than the model grid. These pilot points are spatially connected by a regularisation function; their values are interpolated to the model grid. (4) Inverse modeling of the aquifer parameters is carried out. The reliability of the parameters is demonstrated by two different cross validation methods and different levels of constraining information. Calibrated parameters are assessed with regard to their plausibility and physical meaning. The focus is set to the distribution of the glacial till. (5) Finally, the distribution of the glacial till and the resulting flow field is used to explain hydrochemical observations of redox sensitive species.

2. Material and Methods

2.1. Investigation area

The investigation area is located east of Lake Tegel in the northwest of Berlin, Germany (Fig. 1). Two quaternary aquifers with fine to coarse sand exist. Sieve analyses result in hydraulic conductivities between $1.1*10^{-3}$ ms^{-1} and 10^{-4} ms^{-1} with a mean value of $3*10^{-4}$ ms^{-1}. The upper aquifer has a thickness of 10 m. During the investigation its saturated thickness is spatially and temporally variable, with values between nil and 5m. The lower aquifer has a thickness of 25-30 m. The two aquifers are divided by a glacial till aquitard of 4 m thickness and with a hydraulic conductivity of up to 10^{-9} ms^{-1} (Fritz, 2002), which is very heterogeneously distributed. Information about whether the till is locally existent or not is forthcoming from the borehole logs of five observation wells (diameter 150 mm) and all abstraction wells (diameter 850mm) in this area. The spatial interpretation of this information is shown in Figure 2. In areas where the till exists, the second aquifer can be regarded as confined. In areas where it is nonexistent it can be regarded as unconfined, together with the first aquifer. The aquifer system is sealed at the bottom by thick pleistocene mud and silt layers (Pachur and Haberland, 1977).

Hydraulic heads are recorded hourly in 9 observation wells and in abstraction well 13 (Fig. 2, Fig. 3). The modelling domain has been selected in such a way that short term head variations are modelled correctly. The farther the wells are away from the transect, the less the hydraulic heads react upon well switching. At the transect hydraulic heads in the second aquifer show an immediate reaction of 1 or 2 cm upon switching of well 10 or well 16. This is the lowest detectable head change; the resolution of the data loggers is 1cm. Thus, the distance between the transect and well 10 and 16 (200 m) is defined as the maximum relevant distance. Consequently the outer boundary conditions have a minimum distance to the transect of 200m.

2.2. Flow model

The abstraction creates a cone of depression, inducing large amounts of water infiltrating from Lake Tegel to the first aquifer. In regions where the glacial till is absent water penetrates from the first to the second aquifer, where the wells are screened. About 70% of the abstracted water originates from Lake Tegel, about 30% from the inland subsurface catchment (Wiese, 2006; Massmann et al., 2008, Fritz, 2002)

The flow model is nested inside an existing regional flow model (flow model case3 from Wiese and Nützmann, 2009). Characteristics of both models are listed in Table 1. The outer boundary conditions are extracted from the regional flow model and are introduced by temporal variant 1st type boundary conditions (Fig. 1) using the time-variant specified-head package of MODFLOW2000. The total number of model cells is significantly reduced in order to allow a high temporal resolution (Tab.1). It has to be taken into account that the model has to be run up to several 1000 times during inverse modelling.

The boundary condition representing Lake Tegel is identical to the regional model (Wiese and Nützmann, 2009). It is applied at the interface between aquifer and lake (Figure 3, indicated with dotted line). The reservoir package of MODFLOW2000 is used, it switches between a boundary condition of 2nd type (Neumann type) for unsaturated conditions, and 3rd type (Cauchy type) for saturated conditions. Leakance is temporally and spatially variant.
Between 25 m asl and about 31.4 m asl values increase from $2.3*10^{-7}$ s^{-1} to $3.2*10^{-7}$ s^{-1}. Due to temporally variant clogging effects these values are multiplied by $R_{leak} = f(t)$ with $0.9 \leq R_{leak} \leq 1.8$ (Wiese and Nützmann, 2009). Below 25 m asl limnic mud covers the lake bed (Figure 3, Pachur and Haberland, 1977; Ripl et al., 1987) and inhibits infiltration, hence a no flow boundary is applied.
The wells are screened in the second aquifer. They have an abstraction capacity between 68 and 170 m³/h. Wells are operated discrete, either switched on or off. The switchting periods have a duration between 1 hour and a few days. As an example, the operation pattern of wells 10 to 16 is shown in Figure 4.

2.3. Temporal discretisation

The term “stress period” denotes an interval of boundary condition input. “Time step” is the time discretisation used for the solution of the finite difference groundwater flow equation and the interval between the outputs of hydraulic heads (Harbaugh et al., 2000). The temporal discretisation follows well switching. The length of the stress periods depend on the operation intervals of wells 10 to 16. A new stress period begins, when at least one of these wells is switched. This means, that the model always considers the real operational state of these wells, either switched on or switched off. Wells 6 to 9 and wells 17 to 20 are introduced with daily mean abstraction. The lengths of the stress periods vary between 1 and 24 hours. The time steps are identical to the interval of the secondary observations (see below).

2.4. Hydraulic data and pre-processing

The parameter estimation is based on the short term hydraulic behaviour. The observed heads can not be used in a direct way because they show deviations and offsets larger than the short term structures. This is mainly based on the inaccuracy of calibration of the regional flow model. Handling of the data loggers is another error source. They have been taken out once a month and due to battery lifetime they regularly had to be replaced. This introduced some errors in the reference height, wherefore it was not possible to use the absolute heads. This also prevents that differences between piezometers may be used as secondary observations for calibration.
The abovementioned factors induce a structural misfit, often called structural noise. This structural misfit must not be calibrated within the present model. By pre-processing the hydraulic heads it can be orthogonalised out (Doherty and Welter, 2010). The short term head differences are pre-processed to so--called “secondary observations”.
The present choice of secondary observations has the additional advantage of reducing the computational effort. Two time steps are sufficient for discretisation of a switching period with up to 24 observed heads.
The short term hydraulic behaviour is parameterised using 3 secondary observations. Secondary observation A is used to describe the sharp change in hydraulic heads immediately after the well is switched on or off. It depends principally on the degree of aquifer confinement. Secondary observation B describes the unconfined behaviour, the drawdown is mitigated by the unconfined storage coefficient and because the depression cone is extending. Secondary observation C is just the sum of A and B to maintain the correct shape and overall behaviour (see Fig. 5). The head h_a refers to the last observation before actual well switching, h_b to the observation 2 hours later and h_c to the last observation before the next well switching.

Secondary observation A is calculated as

$$A = h_b - h_a, \quad with\ t_b - t_a = 2h \tag{1}$$

Correspondingly, the secondary observation B and C are calculated according to:

$$B = h_c - h_b\ , \tag{2}$$

$$C = h_c - h_a\ . \tag{3}$$

Between the Mar. 20th and the Oct. 12th 2004 the pattern of well operation for wells 10 to 16 changes n=402 times, providing a lot of information. However, only part of this can be reliably used:

- If the length of interval n is 2 hours or shorter no secondary observation is determined.
- If the length of interval n is 3 hours only secondary observation "A" is determined.
- Sometimes the recorded well switching information contains errors. For some stress periods before and after a detected error no secondary observations are determined.
- For Well 13 secondary observations are only determined if it is not switched itself.
- Logged heads for observation well 3301 and TEG371op do not cover the entire period.

The number of secondary observations which could be determined reliably for each borehole is presented below.

2.5. Error calculation

The temporal discretisation of the model is adapted to the spacing and structure of the head observations and the derived secondary obserations. It has to be taken into account that the logged heads are of hourly interval, but the exact logging time is not known due to inaccuracies in logger time setup. The well switching time is given with hourly precision. In the model, the wells are switched at time t_{s0}, the next time step has a length of 90 minutes and ends at time t_{s1}. The time t_{s2} is the time of the next switching. The observed times t_a, t_b and t_c are estimators for t_{s0}, t_{s1} and t_{s2}. The heads are estimated correspondingly. Although we do not know the individual residuals, their mean is estimated with the following procedure.

The wells are switched at time t_{s0}which is between 0 and 1 hour after t_a, which is the last unaffected observation before the actual switching The probability function of switching time within this interval is assumed to be uniformly distributed, therefore:

$$mean\ \{t_{s0} - t_a\} = 0.5\ \text{h}. \tag{4a}$$

and

$$max\ \{t_{s0} - t_a\} = 1\ \text{h}, \tag{4b}$$

$$min\ \{t_{s0} - t_a\} = 0\ \text{h}, \tag{4c}$$

The head h_a is chosen as estimator for h_{s0}, since the mean of their difference is expected to be zero

$$0 \approx \sum_{i=1}^{N} h_{s0i} - h_{a,i}\ , \tag{5}$$

and because the head change before switching is much smaller than the head change after switching

$$\sum_{i=1}^{N} \left| h_{s0,i} - h_{a,i} \right| << \sum_{i=1}^{N} \left| h_{s1,i} - h_{s0,i} \right|, \tag{6}$$

where h_{s1} is the (unknown) head 90 minutes after well switching. Correspondingly t_{s1} is 90 minutes after t_{s0}. The temporal model discretisation is chosen such because the mean difference between t_b and t_{s1} is nil (Eq. 7).

$$mean\ \{t_b - t_{s1}\} = 0\ \text{h}. \tag{7}$$

The time t_{s2} is close to the end of the stress period n, at the time

$$t_{s2} = t_{s1} + (t_c - t_b)\ . \tag{8}$$

In order to enable calculation of the errors with respect to the interval of the observation data, the secondary observations A, B and C can are expressed as:

$$A = (h_{s0} - h_a) + (h_{s1} - h_{s0}) + (h_b - h_{s1}), \quad (9a)$$

$$B = (h_{s1} - h_b) + (h_{s2} - h_{s1}) + (h_c - h_{s2}), \quad (9b)$$

$$C = (h_{s0} - h_a) + (h_{s2} - h_{s0}) + (h_c - h_{s2}). \quad (9c)$$

The middle parts of Eqs. (9a), (9b) and (9c) represent the unknown reality; the first and the third part have to be introduced as error terms because an uncertainty of 1h exists for the well switching. These expected values of these parts can be approximated as follows:

$$\overline{\nabla h_{ts0-ta}} = \frac{\sum_i \left| h_{a,i} - h_{a-1,i} \right|}{i * 1h}, \quad (10a)$$

$$\overline{\nabla h_{tb-ts1}} = \frac{\sum_i \left| h_{b+1,i} - h_{b,i} \right|}{i * 1h}, \quad (10b)$$

$$\overline{\nabla h_{ts2-tc}} = \frac{\sum_i \left| h_{c,i} - h_{c-1,i} \right|}{i * 1h}. \quad (10c)$$

Where the h_{a-1} and h_{c-1} denotes head observed one hour before h_a and h_c, h_{b+1}denotes the head recorded one hour after h_b. Index i denotes the counter for all positions of a, b and c. In conjunction with equations (9a), (9b) and (9c) the mean error at the times a, b, c can be approximated by:

$$\varepsilon_a = (h_{s0} - h_a) = E(t_{s0} - t_a) * \overline{\nabla h_{ts0-ta}}, \quad (11a)$$

$$\varepsilon_b = (h_{s1} - h_b) = E(t_b - t_{s1}) * \overline{\nabla h_{tb-ts1}}, \quad (11b)$$

$$\varepsilon_c = (h_c - h_{s2}) = E(t_c - t_{s2}) * \overline{\nabla h_{ts2-tc}}. \quad (11c)$$

With

$$E(t_{s0} - t_a) = \frac{1}{i} \sum_i \left| t_{s0,i} - t_{a,i} \right| = 0.5h \quad (12a)$$

$$E(t_b - t_{s1}) = \frac{1}{i} \sum_i \left| t_{b,i} - t_{s1,i} \right| = 0.5h \quad (12b)$$

$$E(t_c - t_{s2}) = \frac{1}{i} \sum_i \left| t_{c,i} - t_{s2,i} \right| = 0.5h \quad (12c)$$

Since ε_a refers to the head slope before actual well switching, it is uncorrelated to ε_b and ε_c. Conservatively, they are treated as if they were positively correlated:

$$F_A = \bar{\varepsilon}_a + \bar{\varepsilon}_b, \quad (13a)$$

$$F_C = \bar{\varepsilon}_a + \bar{\varepsilon}_c. \quad (13c)$$

Since ε_B and ε_C are part of one drawdown or phreatic rise, they have the same direction and are therefore negatively correlated. The error F_B is calculated according to Eq. (13c).

$$F_B = \left| \overline{\varepsilon_b} - \overline{\varepsilon_c} \right|. \quad (13b)$$

The mean error due to the insecurity of parameterisation is obtained by

$$F_{all} = \frac{\sum_{iob} F_A * N(A)_{iob} + \sum_{iob} F_B * N(B)_{iob} + \sum_{iob} F_C * N(C)_{iob}}{N(A) + N(B) + N(C)}, \quad (14)$$

where *iob* is the counter of the observation wells. F_{all} results in 4.9 mm. The individual errors are listed in Tab. 3.

2.6. Spatial model parameterisation

In order to assign spatial information to the entire model, pilot points with triangular linear interpolation are used (Certes and Marsily, 1991). A pilot point consists of a spatial position and one or more parameter values. The pilot point values are transferred to the model grid spatially by means of a triangular grid, each edge of a triangle is formed by a pilot point (Fig. 6).

The area around the transect is of primary interest, therefore the finest discretisation can be found here and only here the Delaunay condition is fulfilled, i.e. there is no further point within a circle through the edge points of a triangle (Fig. 6). In regions of low information and secondary interest each pilot point affects a much larger area and the Delauney condition is not necessarily fulfilled. Each borehole, which is penetrating the aquitard, is respected as a pilot point.

The spatial parameterisation using the pilot points is applied to the 4 most relevant parameters:

- [L:] Leakage of the glacial till
- [S:] Unconfined storage coefficient
- [Hk1:] Horizontal hydraulic conductivity aquifer 1
- [Hk2:] Horizontal hydraulic conductivity aquifer 2

Pilot point values are triangulated to the model grid, logarithmically for L, Hk1 and Hk2 and linearly for S.

The leakage of the glacial till is conditioned based on the observed distribution of the glacial till. In boreholes where the glacial till is existent with at least 2m thickness (Wells 6, 7, 8, 9, 10, 12, 13, 15, 16, 18, observation wells 3302, 3303, 3304) the leakage is constrained to 10^{-9} s^{-1}. The observation wells have a diameter of 100 mm; the wells have a diameter of 850mm. The larger the diameter of the borehole is, the higher the probability that tiny till layers may not have been recognised during drilling.

The diameter of the boreholes implies that tiny till layers may exist which have not be recognised during drilling. Consequently, pilot points are unconditioned when pertaining to boreholes in which no till or only tiny till is found. Also all other pilot points are modelled unconditioned.

The leakage parameters are constrained such that they can represent all states between a fully expressed glacial till with a hydraulic conductivity of $5*10^{-9}$ ms^{-1} and pure aquifer sand with $5*10^{-4}$ ms^{-1}, the leakage may take values between $10^{-9}s^{-1}$ $10^{-4}s^{-1}$. The lower bound of the horizontal hydraulic conductivity is set to $3*10^{-5}$ ms^{-1}, the upper bound $3*10^{-3}$ ms^{-1}. In order to detect overfitting, the bandwidth is one order of magnitude larger than observed local values (Ripl et al., 1987).

Other aquifer parameters are:

- Vertical hydraulic conductivity of both aquifers: $8*10^{-5}$ ms^{-1}
- Horizontal hydraulic conductivity glacial till: 10^{-8} ms^{-1}
- Confined storage coefficient: 10^{-5} [-].

It is not necessary to estimate the vertical hydraulic conductivity of the aquifers because the vertical flow is controlled by the glacial till. Since the confining layer is modelled explicitly, the confined storage coefficient is considered as constant with its physical value.

2.7. Inverse method

Inverse modelling is carried out with PEST (Doherty, 2004). In contrast to other inverse modelling codes it offers the possibility of regularisation. Regularisation information makes the inversion a constraint optimisation, similar to use "ordinary" prior information. The difference is that the regularisation information has a deeper rank than the measurement objective function,

$$\Phi_{tot} = \gamma\Phi_{obs} + \Phi_{reg}, \quad (14)$$

where Φ_{tot} is the objective function which shall be minimised, γ is the Lagrange multiplier, Φ_{obs} is the observation part of the objective function, and Φ_{reg} is the contribution of the regularisation. The task is to minimise Φ_{tot}, which means that it decreases or stays constant

$$\Phi_{tot} \leq \Phi^1_{tot}, \quad (15)$$

where the upper index 1 indicates the last iteration. The Lagrange multiplier γ is chosen such that

$$\Phi_{obs} \leq \Phi^1_{obs}, \quad (16)$$

where Φ^1_{obs} is the measurement objective function of the last iteration. Setting a target value for the measurement objective function slightly above minimum allows determining the impact of the regularisation function on the parameters and as a criterion whether calibration is based on (structural) noise. However, in the current approach the noise is accounted for by resampling. If the noise persist the resampling method it probably would also persist a target measurement objective function. The objective function of the measurements is calculated by

$$\Phi_{obs} = \sum_{i=1,N} (w_i\, r_i)^2, \quad (17)$$

where N is the number of observations, w_i the weighting factor. In the current study the residuals are equally weighted, all w_i are 1. The residuals r are calculated as

$$r = o - s \quad (18)$$

where s is the simulated value and o the observation.

The pilot points are spatially constrained by a smoothing regularisation:

$$\Phi_{reg} = \sum_{i=1}^{n} \sum_{j=1}^{k(i)} \left| \log(PP_i) - \log(PP_j) \right|, \quad (19)$$

where n is the number of pilot points with i as counter, $k(i)$ is the number of neighbours of each pilot points. The values of the regularisation function may increase or decrease for each iteration. For further information refer to Doherty (2004).

In order to assess the inversion stability and therefore the physical relevance of the calibrated parameters, the model is calibrated with different subsets of input data and different initial conditions. The 8 different configurations are presented in Table 2. Except for the leakage, initial aquifer conditions are homogeneous.

2.8. Geochemistry

The redox sensitive species oxygen, nitrate, manganese, iron and ammonium have been sampled each month between January 2003 and August 2004 in observation wells 3301, 3302, 3303, TEG371op, TEG371up and TEG372. O_2 is measured with an oxygen electrode in a flow through cell during sampling. The other species are determined in the laboratory, NO_3^- according to DIN EN ISO 10304-1/2, Fe^{++} and Mn^{++} according to DIN EN 11885 (E22), $NH4^+$ according to DIN 38406-E05-1. Observation wells 3301, 3302, 3303, TEG371op, TEG371up and TEG372 are chosen because they show 100% bank filtrate (Pekdeger, 2006; Fritz 2002).

3. Results and Discussion

3.1. Hydraulic Inversion

3.1.1. Unconfined Storage Coefficient

At inversion C1 all 4 aquifer parameters have been calibrated simultaneously. In large areas the unconfined storage coefficient hits the imposed boundaries of 0.1 and 0.3 [-]. This contradicts as well the general hydrogeologic situation in the aquifer and as well the specific bore profiles or grain size distributions at the particular boreholes. While storage is believed to have a relatively homogeneous distribution, the estimated storage is strongly heterogenous

because it is correlated to transmissivity and therefore frequently subject of overfitting (Meier et al. 1998, Cirpka et al. 2006). We conclude that the calibrated strongly heterogeneous storage coefficient is result of overfitting. Therefore, instead a constant unconfined storage coefficient of 0.21 is applied for all subsequent inversions. This value corresponds to the geological profiles (Voigt and Eichberg, 2000), grain size distributions (Fritz, 2002), TDR measurements in the same area (Greskowiak et al., 2005), and groundwater modelling (Wiese and Nützmann, 2009).

3.1.2. Cross Validation

The reliability of the parameters horizontal conductivity in aquifer 1 and 2 and till leakage is assessed by temporal re-sampling. Three calibrations (C2, C3, and C4) are carried out. The calibration C2 is based on the entire data set, the calibration C3 is based on data before between 20th March and 30th June, the calibration C4 is based on data between 1st July and 12th October. Since not all observation well data cover the entire model period, the temporal segmentation of the observations also means a shift between observation wells. C3 only comprises 4 weeks of observation well 3304, C4 only comprises 6 weeks of 3301 and no data of TEG371op. A further difference is the different hydraulic situation. The observed heads are in average about 1.5 m higher during C3 (first part) than during C4 (second part). The difference is underestimated by the model (Figure 11). The modelled heads at the transect during C3 tend to be up to 0.5 m lower than observed (positive residuals, Eq. 18), during C4 they tend to be up to 0.5 m higher than observed (negative residuals).

All three calibrations show large areas with aquifer conductivities slightly outside the range of sieve analyses between 10^{-4} and 10^{-3} (Fig. 7). This is a hint that calibrated conductivities may not be physically based. Moreover, the resulting spatial distributions are considerably different for all three calibrations. This is a hard indication, that hydraulic conductivity can not be calibrated in a physically meaningful way.

In contrast to that, the leakage of the glacial till shows quite similar distributions for C2, C3 and C4 (Fig. 7). The till is expressed continuously with holes in the structure. One big hole exists north of the transect between the well field and the lake, a smaller inland of the well field south of the transect.

The inversion stability of the glacial tills spatial structure is demonstrated by 3 further cross validation runs C5, C6 and C7. The model is calibrated using the entire period, but each run only is calibrated to the secondary observations A, B or C. Unconfined storage coefficient is set to 0.21, horizontal conductivity to $3.5*10^{-4}$ for both aquifers. Initial leakage distribution is taken from calibration run C2. The results are shown in Fig. 8. The differences between these runs are higher than for temporal cross validation, but close to the transect the structure of a continuous glacial till with two holes is very similar (Fig. 8).

The impact of constraining the leakage is assessed with inversion C8 where the leakage is not constrained to the existence of the glacial till. Results (no figure) are very similar to results of C2, the shape of the aquitard structure is slightly different, but the main difference is that the minimum leakage is 10^{-7} s^{-1}. Values do not become as low as 10^{-9} s^{-1} because hydraulically the vertical exchange becomes insignificant compared to horizontal exchange.

Calibration with different subsets of observations and model parameterisation shows great similarities in the distribution of the glacial till close to the transect. Based on interpretation of the different scenarios, 1% of the maximum sensitivity can be regarded as the threshold value for physically meaningful calibration (Fig. 9). The area of sensitivity is asymmetric to the transect. Its extent is larger to the lake than inland and larger to the north than to the south. This is caused due to the distribution of observation wells. It is remarkable, that observation well 3313 extends the sensitive regions significantly to the north and provides sensitive information about the distribution of the glacial till though it is screened above the till in the first aquifer.

The glacial till also appears to exist below the lake. The exact position of holes and till can not be determined because results differ for different calibration runs. But for all runs the leakage is considerably lower than 10^{-4} s^{-1} which indicates that some extend of till exists.

3.1.3. Comparison with borehole profiles

The calibrated leakage is compared with the bore profiles. At wells 11 and 14 till has not been found. Leakage here is calibrated to have values around 10^{-5} s^{-1} to 10^{-6} s^{-1}. This indicates reasonable semi confined conditions like they occur when the till is expressed discontinuously or only with small thickness. Since the wells have diameters of 850 mm tiny till layers are not detected during drilling. The observation wells are drilled with a diameter of about 150 mm, which allows higher resolution of the bore profile. At observation well 3301 a till layer with a thickness of 10 cm is found, corresponding well to the calibrated leakage of 10^{-6} s^{-1}. Eight metres away, the bore profile of TEG371up does not indicate any glacial till, which coincides with the calibrated leakage of 10^{-4} s^{-1}.
The calibrated leakage with the unconstrained inversion C8 also roughly approves the observed distribution of the glacial till. The main difference occurs at observation well 3302 and abstraction well 12. Here 4 m till is found in the bore profile, but the model result only show semi confined conditions (leakage of 10^{-6} s^{-1}).

3.1.4. Model fit

The model fit is presented for results of inversion C2. Observed and simulated hydraulic heads coincide very well (Fig. 10). The absolute value of the mean deviation is 23 mm, the regression coefficient is R^2=0.987. The model is calibrated to the minimisation of the squared residuals, which means that results are independent of the magnitude of the observations; the absolute bandwidth of the residuals is rather independent of the magnitude of the corresponding observation. The dynamic of simulated and observed hydraulic heads show an excellent match. Though only about 30% of the switching periods have been used for calibration, also the other differences match very well (Fig. 11).

3.1.5. Error calculation

The mean errors for each secondary observation at each observation well are presented in Tab. 3. The mean errors F_A, F_B and F_C are always less than 10mm with a mean of 4.6 mm. F_B are considerably smaller than for F_A and F_C because the 2 heads between which B is calculated, both lie on the same limb, thus errors partly eliminate (Eq. 13c). For all secondary observations (A, B, C) the deviations are small in relation to their magnitude, usually around 3% (Tab. 3). Higher errors only occur at shallow observation wells, where the magnitude of the head change is lower. The relative error for A is particularly high here, since the unconfined conditions cause a lower variation of A. The contribution to the error in the calibrated model also is acceptable. The mean of the residuals of the calibrated model C2 is 23 mm, much higher than the 4.6 mm of error (Eq. 14) introduced due to the insecurity in temporal resolution.

3.2. Geochemistry

3.2.1. Observations

The observed concentration of redox sensitive species however shows some particularities. One would expect that the redox state decreases with distance to the bank and with the depth of the observation well. As expected, the shallow observation wells TEG371op and TEG372 are screened above the glacial till and have a much higher redox state than the other observation wells which are deeper (Tab. 4). However, redox values are slightly reversed with respect to their distance to the bank. Observation wells 3301, 3302 and 3303 are screened in

similar depth with increasing distance to the shore, but the redox state is lowest in 3301. The lowest redox state can be found in TEG371up though the screen is located higher than for 3301, 3302, 3303 and closer to the bank than 3302 and 3303. Sedimentary organic carbon concentrations in TEG371up are not higher than in the other observation wells (Pekdeger, 2006).

3.2.2. Hydraulic context

Prior to characterising how the glacial till impacts redox conditions, it is necessary to understand the redox conditions during infiltration. As a consequence of a highly variable groundwater table, oxygen intrudes into the unsaturated zone below the infiltration area. The infiltrated water partly is reoxidised and close to the bank redox conditions are higher than farer away (Pekdeger, 2006; Wiese and Nützmann, 2009). The reduced water from farer away stratifies below the oxic water (Wiese, 2006). Furthermore, during increasing water table air is entrapped which provides an oxygen source in shallow groundwater (Massmann and Sültenfuß, 2008). These processes cause vertically stratified redox conditions.

Below the lake a glacial till layer exists, with water of low redox directly above and increasing redox state at higher elevation. At the location of TEG371up the till has a hole while it is present only 8 m away at observation well 3301. TEG371up is just at the border of the hole, where the reduced water from just above the till flows downwards (Fig. 12). As consequence TEG371up shows the lowest redox state of all observation wells.

The redox gradient in combination with the holey structure of glacial till induce a reversed redox state at observation wells 3301, 3302 and 3303 with regard to their distance to the bank (Pekdeger, 2006; Wiese, 2006). Unless a cross sectional interpretation of the transect may suggest, 3302 and 3303 do not lie on the same flow path, as indicated by the bent arrows in Figure 12. Water sampled in 3303 has been exposed longer to reoxidation, also at lower total nitrogen content than in 3302 (Tab. 4). Though water in 3303 is older than in 3302 (Massmann et al., 2008), transport simulation shows that the residence time in the second aquifer is identical (Wiese, 2006). Observation well 3301 is also affected by more regional flow and thus can not be interpreted in detail here, but the mechanisms are similar. A full interpretation is given in Wiese (2006).

In an unconfined aquifer Bourg and Bertain (1993) interpreted increasing redox values of groundwater approaching a well field in a similar way concerning re-oxidation. The present study shows that similar effects may occur in aquifers which appear to be confined.

4. Conclusions

4.1. Hydraulic calibration

The method presented here is suitable to determine the spatial distribution of an aquitard in the vicinity of abstraction wells. The calibration results are very accurate with regard to temporal dynamics though the hydraulic model and observation data have inaccuracies which are common in field studies. The error introduced due to observations with hourly precision is uncritical, since it is much smaller than the mean of the residuals. The short term head differences are only calculated within each time series because these are not susceptible to common measurement errors such as reference level or logger drift.

The inversion is not stable with regard to unconfined storage coefficient and aquifer hydraulic conductivity. The unstable aquifer conductivity does not affect significantly the calibrated till structure. The leakage shows a physical variation by five orders of magnitude while the hydraulic conductivity varies only by one order of magnitude.

In the center of the investigation area the calibrated leakage is physically meaningful. The correctness of the calibrated glacial till pattern is approved by two cross validation procedures. Also unconditioned results are consistent with glacial till distributions found in

bore profiles. The leakage calibration is robust, and is not susceptible to inaccuracies which occur in modeling practice.
The calibrated distribution of the glacial till is substantially different from the interpretation solely based on evaluating the existence in bore profiles. In contrast to the previous assumption the till is present in large areas between the well field and the lake and even below the lake. The area with till are larger than the area without. With the present regularisation method this leads to the spatial structure that the till forms the continuum and areas where the till is not existent are isolated.
With existing observation wells data can be acquired relatively cheap. The method shows a way to process large amounts of operational data without early aggregation in order to obtain specific knowledge about subsurface properties. Stochastic data or assumptions about the aquifer structure are not required. A special benefit is that shallow observation wells provide sensitive information about the aquitard below.

4.2. Redox conditions

Only the calibrated distribution of the glacial till allows a consistent interpretation of the geochemical data. The discontinuous distribution of the glacial till strongly affects the flow field. As consequence the redox conditions can not be easily predicted and appear contradictory. The low redox state of TEG371up can only be explained by the glacial till deflecting the redox stratified groundwater. The calibrated till distribution also allows to interpret increasing redox conditions due to aquifer specific residence time, which is not possible with interpreting flow path based on a cross section.

5. Outlook

The method appears applicable to other field sites. For a successful transfer one has to consider the advantages of the present field site:

- the high capacity of abstraction wells
- highly transient flow field
- many observation wells
- defined elevation of aquitard

However, conditions are substantially different to a synthetic test case, and the method has proven to cope with the adverse conditions:

- significant offset of hydraulic model
- unknown precision of head observations and pumping rates
- some errors in pump switching data

Simulating in an area where the regional flow field is defined better, the method may also produce sensitive results for aquifer parameters hydraulic conductivity and unconfined storage coefficient. A higher temporal precision in data logging would reduce the pre-processing effort and increase accuracy. Including also other kind of information, such as differences between different observation wells or even transport data, would increase the accuracy.
It might be possible also to calibrate hydraulic conductivity or unconfined storage coefficient. To achieve this, the quality of regional hydraulic model should be increased. As well the data regarding temporal resolution and differences between different observation wells. Coupling with transport modelling is possible.

Acknowledgements

This work was carried out in the NASRI project, funded by KompetenzZentrum Wasser Berlin, Berlin Water Works and Veolia Water. Comments by John Doherty have helped to improved the final text and are gratefully acknowledged. The authors are grateful to Berlin

Water Works and Gudrun Massmann (Free University Berlin) for providing the hydraulic data.

References

Alcolea, A., Renard, P., Mariethoz, G.,Bertone, F., 2009. Reducing the impact of a desalination plant using stochastic modeling and optimization techniques. Journal of Hydrology 365 (3-4), 275-288.

Bourg, A.C.M. and Bertin, C. 1993. Biogeochemical processes during the infiltration of river water into an alluvial aquifer. Environmental Science and Technology 27(4), 661-666.

Certes, C.and DeMarsily, G. 1991. Application of the pilot point method to the identification of aquifer transmissivities. Advances in Water Resources 14 (5): 284-300.

Cirpka, O A, Li, W, Englert, A. 2006 Hydraulic tomography and the Curse of Storativity, American Geophysical Union, Fall Meeting 2006.

Datta, B., Chakrabarty, D.,Dhar, A., 2009. Simultaneous identification of unknown groundwater pollution sources and estimation of aquifer parameters. Journal of Hydrology 376 (1-2), 48-57.

Diersch, H. 1998. FEFLOW user's manual - interactive, graphics-based finite element simulation system for modeling groundwater flow, contaminate mass and heat transport processes. WASY Institute for Water Resources Planning and Systems Research Ltd.

Dingman, S.L. 2008. Physical Hydrology, Second Edition (reissued), Waveland Press Inc. 646 pp.

Doherty, J. 2004. Pest - Model-Independent Parameter Estimation, User Manual: 5th Edition: 336 pp.

Doherty, J., Welter, D., 2010. A short exploration of structural noise. Water Resources Research 46, W05525.

Feyen, L., Caers, J., 2006. Quantifying geological uncertainty for flow and transport modeling in multi-modal heterogeneous formations. Advances in Water Resources 29 (6), 912-929.

Fritz, B. 2002. Untersuchungen zur Uferfiltration unter verschiedenen Wasserwirtschaftlichen, Hydrologischen und Hydraulischen Bedingungen, PhD thesis (in German) Free University Berlin, Berlin, 203 pp.

Gedeon, M., Wemaere, I. and Marivoet, J. 2007. Regional groundwater model of north-east Belgium. Journal of Hydrology 335, 133-139.

Greskowiak, J., Prommer, H., Massmann, G., Johnston, C.D., Nützmann, G. and Pekdeger, A. 2005. The impact of variably saturated conditions on hydrogeochemical changes during artificial recharge of groundwater. Applied Geochemistry 20(7), 1409-1426.

Harbaugh, A.W., E.R. Banta, M.C. Hill, and M.G. McDonald. 2000. MODFLOW-2000, The U.S. Geological Survey modular ground-water model. User guide to modularization concepts and the ground-water flow process. Open-File Report 00–92. Hunter, Kansas: USGS.

Krabbenhoft, D.P. and M.P. Anderson. 1986. Use of a numerical ground water flow model for hypothesis testing. Ground Water 24 (1), 49-55.

Leake, S. A. and Claar, D. V. 1999. Procedures and Computer Programs for Telescopic Mesh Refinement using MODFLOW. Open-File Report 99-238. U. S. G. Survey. Tucson, Arizona.

Machado, C., Santiago, M., Mendonça, L., Frischkorn, H., and J. Filho Mendes. 2007. Hydrogeochemical and flow modeling of aquitard percolation in the Cariri Valley – northeast Brazil. Aquatic Geochemistry 13 (2) 187-196.

Martin, P. J. and E. O. Frind. 1998. Modeling a complex multi-aquifer system: the Waterloo Moraine. Ground Water 36(4) 679-690.

Massmann G, Sültenfuß J, Dünnbier U, Knappe A, Taute T, Pekdeger A. 2008 Investigation of groundwater residence times during bank filtration in Berlin: A multi-tracer approach. Hydrological Processes. 22 788-801.

Massmann G, Sültenfuß J. 2008 Identification of processes affecting excess air formation during natural bank filtration and managed aquifer recharge. Journal of Hydrology.

Meier, P. M., Carrera, J.,Sanchez-Vila, X., 1998. An evaluation of Jacob's method for the interpretation of pumping tests in heterogeneous formations. Water Resources Research 34 (5), 1011-1025.

Pachur, H. J., and W. Haberland. 1977. Untersuchungen zur morphologischen Entwicklung des Tegeler Sees. Die Erde 108 no. 4, 320-341.

Parkhurst, D. L., Appelo, C. A. J., 1999. User's Guide to PHREEQC (Version 2) - a computer program for speciation, batch-reaction, one-dimensional transport, and inverse geochemical calculations. USGS Water-Resources Investigation Report 99-4259.

Pekdeger A. 2006 Hydrogeological-hydrogeochemical processes during bank filtration and ground water recharge using a multi tracer approach. NASRI - Final Project Report. Freie Universität Berlin, Berlin, pp. 176.

Ripl, W., Heller, S. and Linnenweber, C. 1987. Limnologische Untersuchungen an den Sedimenten des Tegeler Sees, Technische Universität Berlin, Berlin.
Rötting, T. S., J. Carrera, B. J., and S. J.M. 2006. Stream-stage response tests and their joint interpretation with pumping tests. Groundwater 44 no. 3: 371-385.
Timms, W. A. 2001. The importance of aquitard windows in the development of alluvial groundwater systems: Lower Murrumbidgee, Australia. PhD thesis, University of New South Wales, http://handle.unsw.edu.au/1959.4/18671.
Voigt, I. and Eichberg, M. 2000. Hydrogeologische Übersichtsprofile Nr.1-Nr.10, erstellt von der Fugro im Auftrag der BWB, Berlin.
Wiese, B. 2006. Spatially and temporally scaled inverse hydraulic modelling, multi tracer transport modelling and interaction with geochemical processes at a highly transient bank filtration site, PhD thesis, Humboldt-University Berlin, Berlin, 155 pp.
Wiese, B., and Nützmann, G. 2009. Transient leakage and infiltration characteristics during lake bank filtration. Ground Water 47 (1), 57-68.

Figures

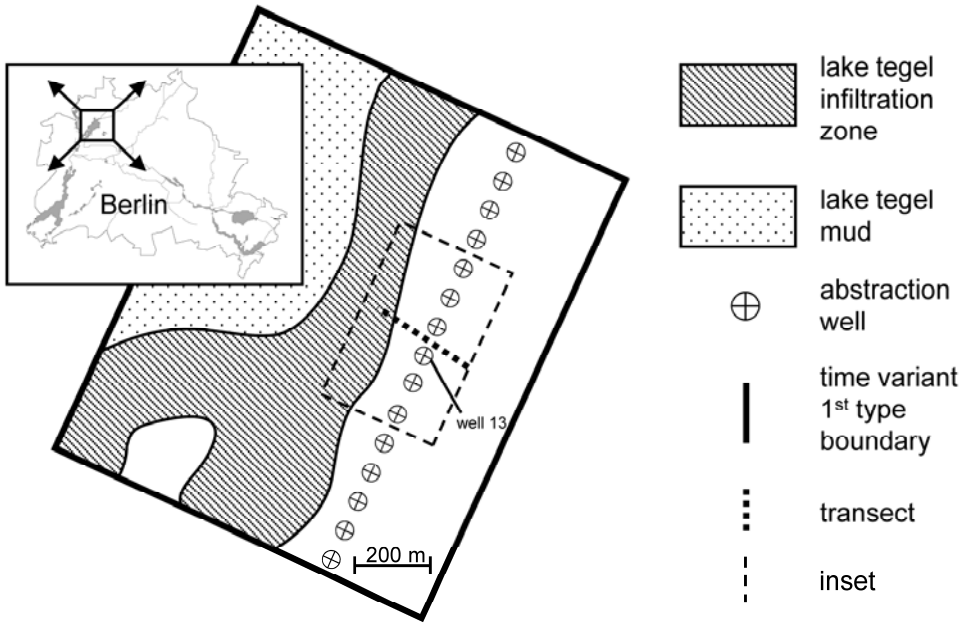

Fig. 1: Investigation area and model domain. Outer boundary conditions are extracted from a regional flow model (Wiese and Nützmann, 2009)

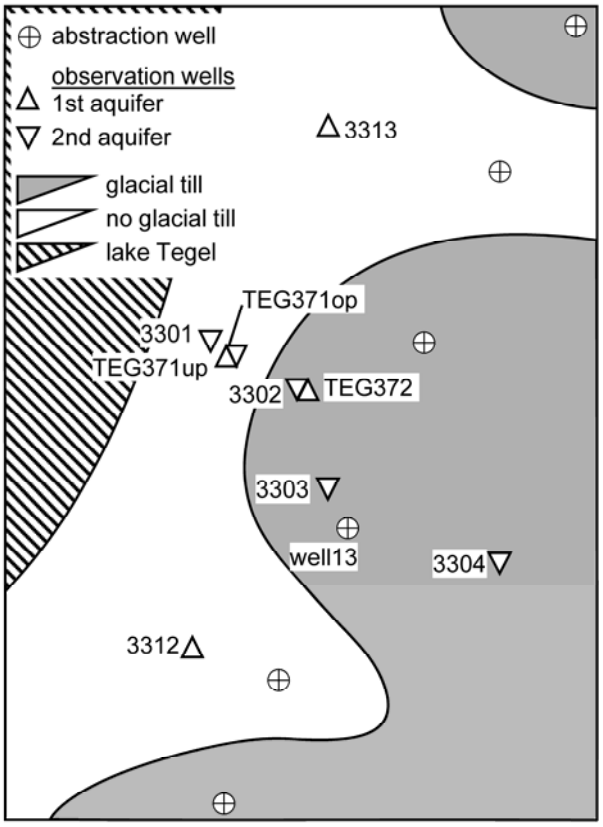

Fig. 2: Transect of observation wells and centre of investigation area. Heads are logged in all observation wells and abstraction well 13. Only the observation wells which are screened in the second aquifer and the abstraction wells penetrate the stage of the glacial till. The interpretation of the distribution of the glacial till follows Fritz (2002) and Voigt and Eichberg (2000)

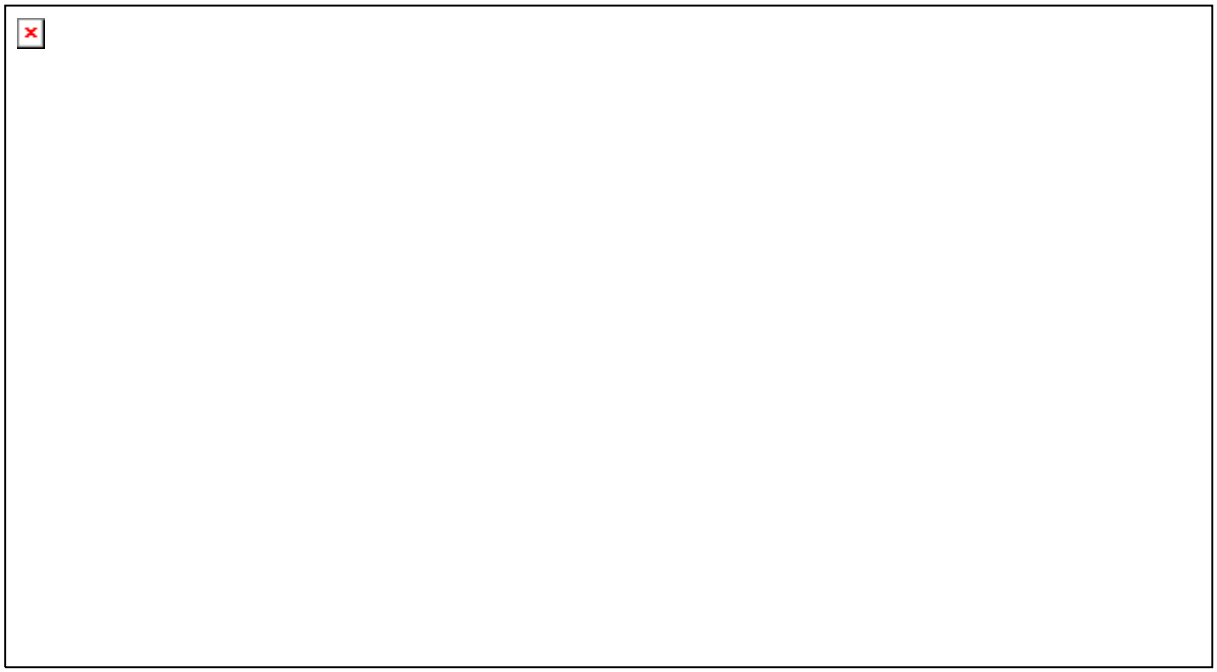

Fig. 3: Cross section at the transect. The interpretation of the distribution of the glacial till follows Fritz (2002) and Voigt and Eichberg (2000)

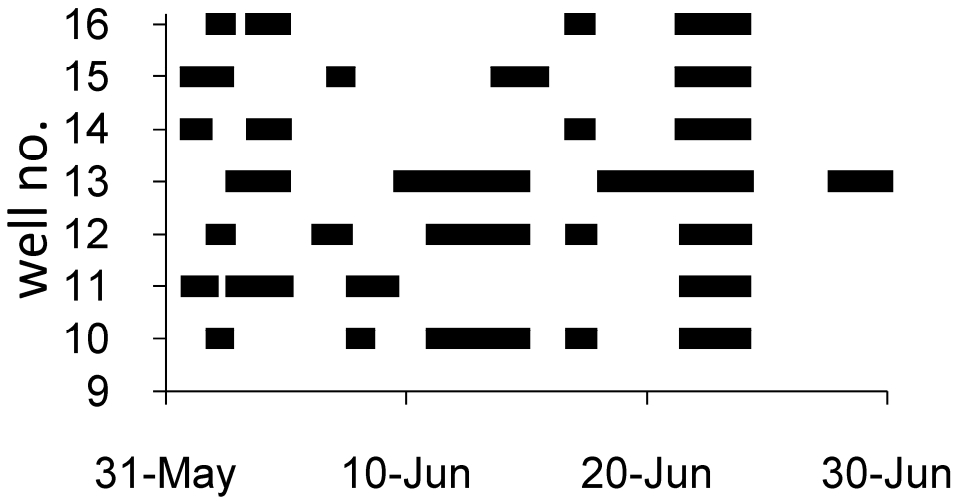

Fig. 4: Operational scheme of wells 10 to 16 in June 2004. Black lines indicate the corresponding well which is switched on.

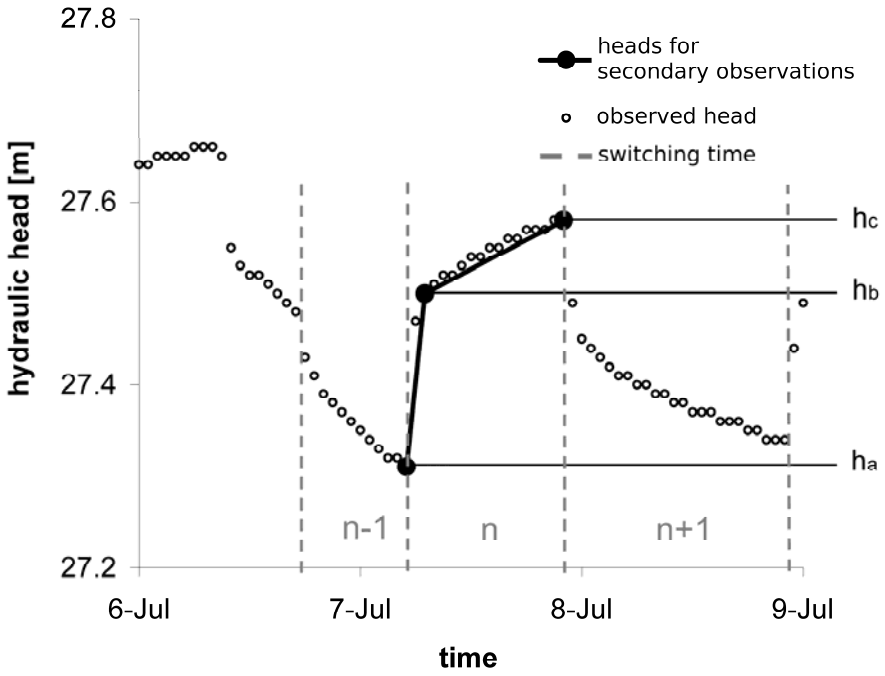

Fig. 5: The small circles shows measured hydraulic heads, the large black circles show the heads which are used for the generation of secondary observations. The discretization interval is indicated by n. The time t_a and head h_a correspond to the last observed head of the previous stress period n-1, t_b and h_b correspond to the observed head 2 hours after t_a. The last observed head of the stress period is represented by t_c and h_c.

Fig. 6: Location of the pilot points. Black circles indicate pilot points at the location of deep boreholes, line connections represent the other pilot points. The black lines show the interpolation triangles.

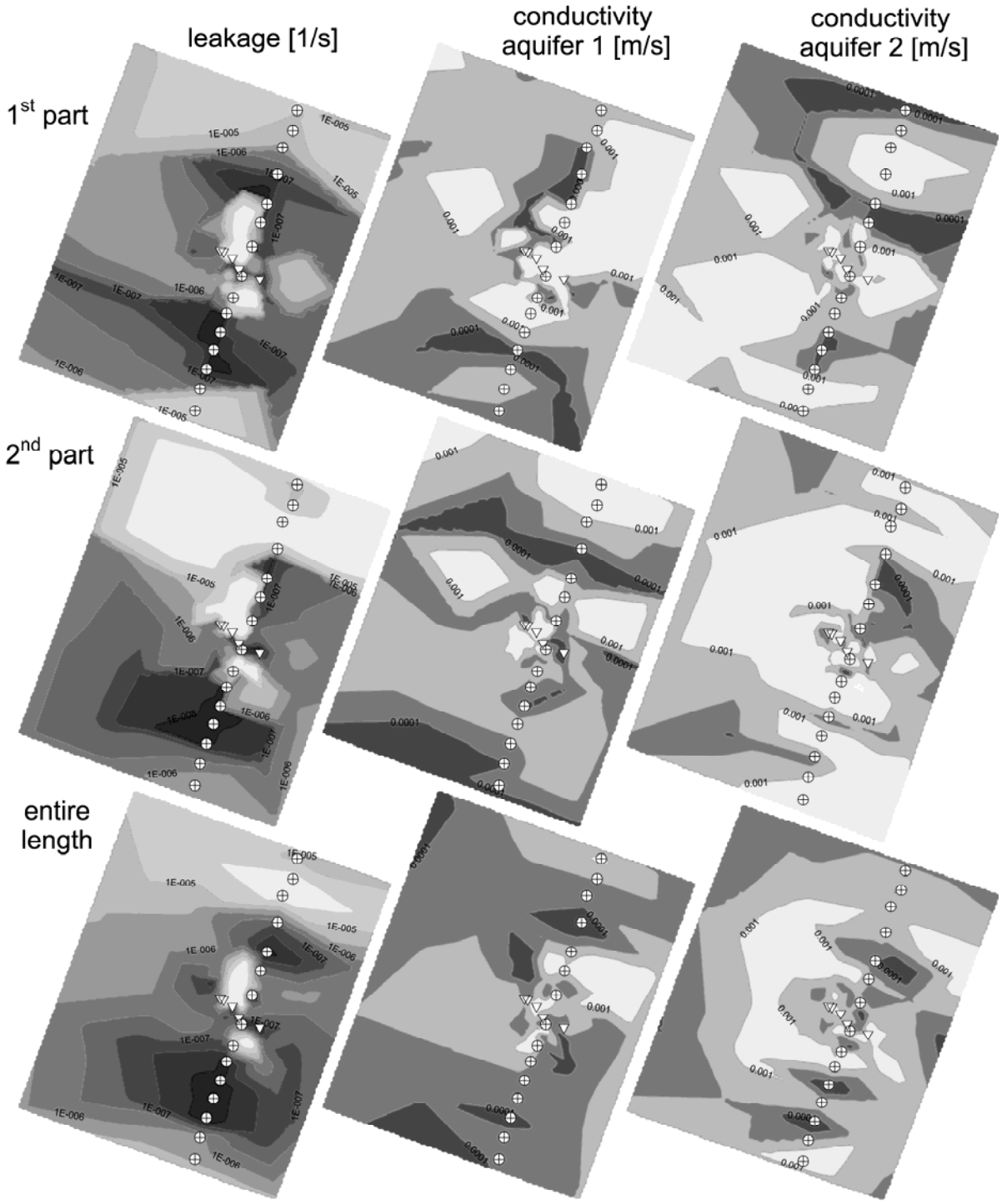

Fig. 7: Calibration results using different temporal subsets of observations. The elements of the first row are calibrated only using observations until the 30th June (C3); the second row is calibrated only using observations after the 1st of July (C4). The last row is calibrated with the entire data set (C2). The columns correspond to leakage, conductivity of aquifer 1 and conductivity of aquifer 2. The crossed circles represent abstraction wells, the triangles deep observation wells.

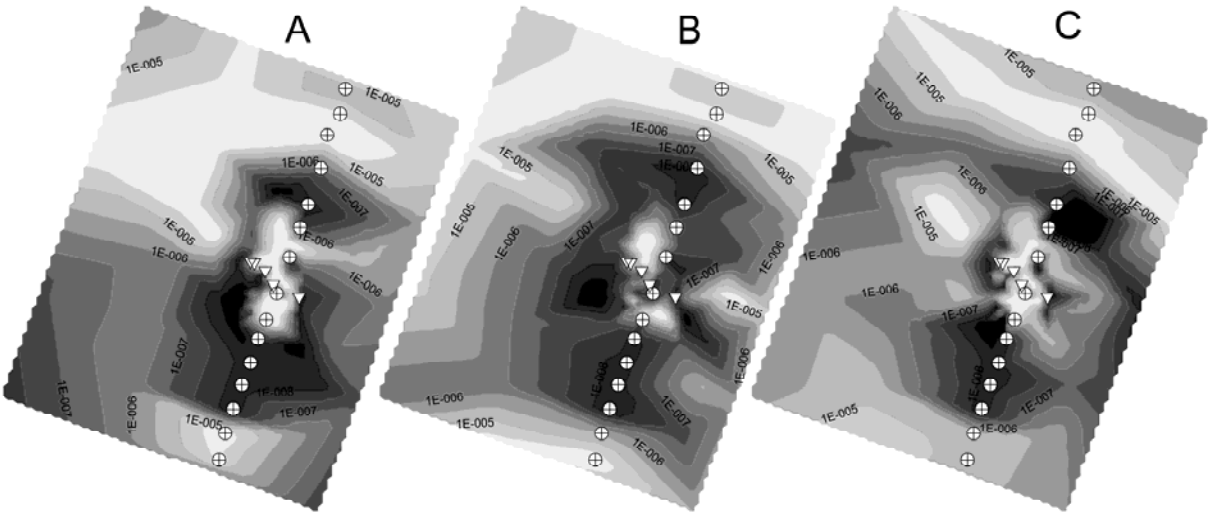

Fig. 8: Calibrated leakage of the glacial till using subsets of the observations, containing only secondary observations A, B and C. The red dots indicate boreholes which penetrate the glacial till. The grey scale indicates the leakage.

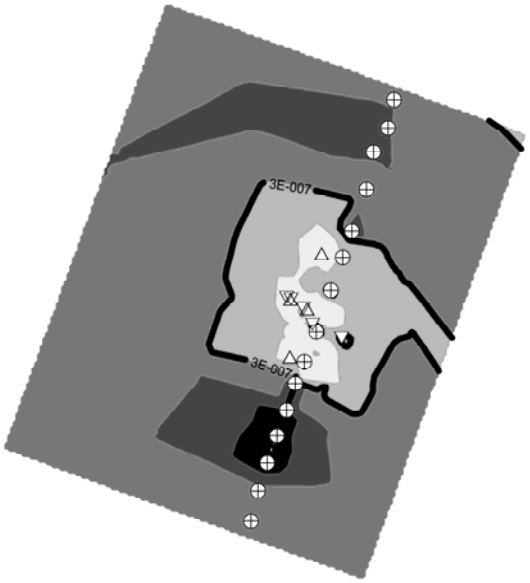

Fig. 9: Sensitivity of the glacial till from inversion C2. The sensitivity of each pilot point is divided by the area it affects and interpolated to the area. The thick line shows 1% sensitivity. Comparison with Fig. 7 and Fig.8 this can be regarded as outer boundary for sensitive glacial till calibration. The small regions of low sensitivity arise, because the leakage at the corresponding pilot points is fixed.

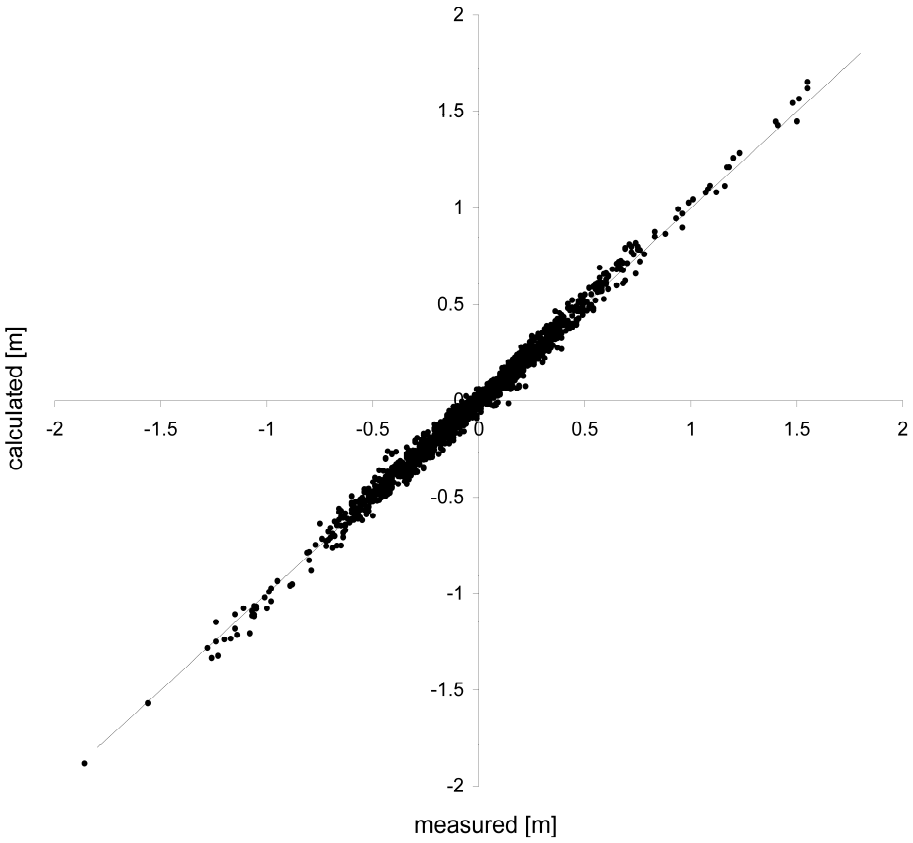

Fig. 10: Calibrated versus secondary observations A, B and C. The mean of the absolute residual is 23 mm, the regression coefficient $R^2 = 0.987$.

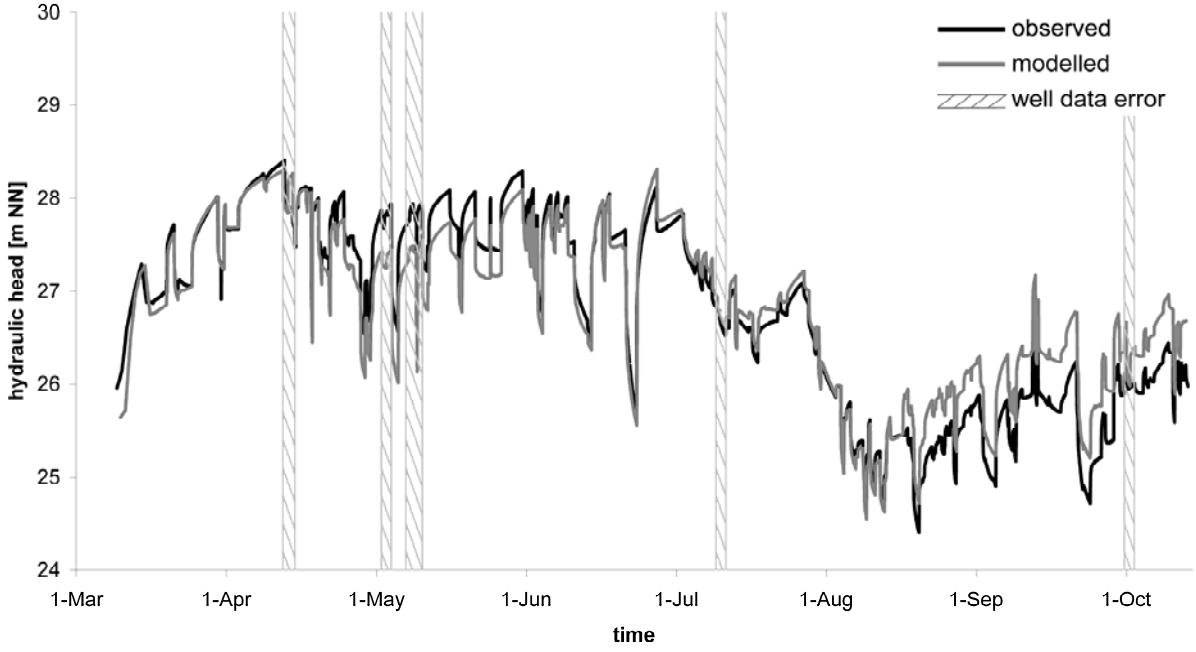

Fig. 11: Simulated and measured curves of hydraulic heads in observation well 3302. The grey lines indicate periods when the recorded well switching times are not correct.

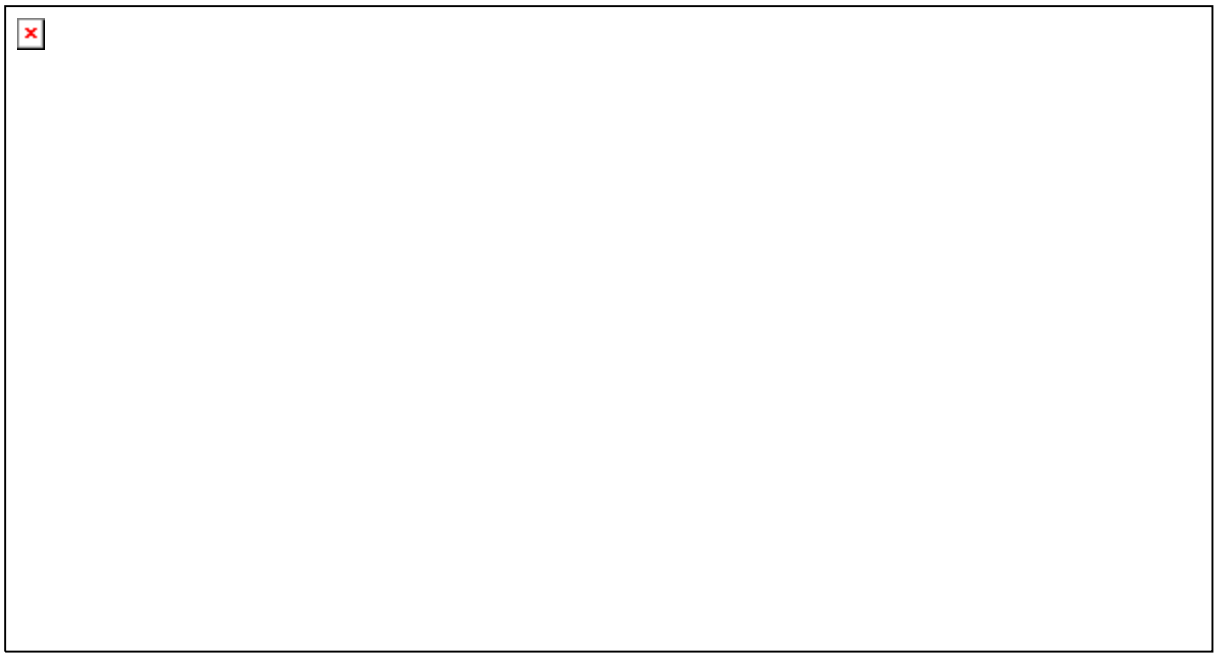

Fig. 12: Cross sectional scheme of the hydraulic situation section of the transect considering the calibrated distribution of the glacial till. Arrows indicate magnitude and direction of subsurface water flow. Bend arrays across the till indicate flow paths on another plane, behind the current cross section. Question marks indicate the area where the aquitard generally exists, but the exact position of the holes is unknown.

Tables

parameter	regional model	local model
temporal discretization	1 week	1-24 hours
begin	1-Jan-1998	10-Mar-2001
duration	7.3 years	218 days
stress periods	370	414
time steps	370	1177
cells	142506	32256
finest discretization (row*col)	5*5 m	5*5 m
coarsest discretization (row*col)	15*50 m	15*25 m
model domain	4.3 km²	0.65 km²
layers	7	6
wells	27	15

Tab. 1: Model characteristics of the regional model (Wiese & Nützmann, 2009) and the local model used in this study.

inversion no.	observation parameters	observation time	calibrated aquifer parameters	constrained leakage	initial leakage
C1	A,B, C	entire period	Hk1, Hk2, L, Sc	Yes	10^{-4}
C2	A,B, C	entire period	Hk1, Hk2, L	Yes	10^{-4}
C3	A,B, C	first half	Hk1, Hk2, L	Yes	10^{-4}
C4	A,B, C	second half	Hk1, Hk2, L	Yes	10^{-4}
C5	A	entire period	L	Yes	from C2
C6	B	entire period	L	Yes	from C2
C7	C	entire period	L	Yes	from C2
C8	A,B,C	entire period	Hk1, Hk2, L	No	from C2

Tab. 2: Setup of the calibration runs. Aquifer parameters Hk1 and Hk2 denote hydraulic conductivities in aquifer 1 and 2, L denotes the leakage of the till, Sc denotes unconfined storage coefficient. Initial leakage refers to unconstrained pilot points. Inversion C2 is the reference case.

obs. well	$N(A)$	$N(B,C)$	$\overline{\nabla h_{ts0-ta}}$ [mm/h]	$\overline{\nabla h_{tb-ts1}}$ [mm/h]	$\overline{\nabla h_{ts2-tc}}$ [mm/h]	$\overline{A}$ [mm]	$\overline{B}$ [mm]	$\overline{C}$ [mm]	ε_A [mm]	ε_B [mm]	ε_C [mm]	F_A [mm]	F_B [mm]	F_C [mm]	$\frac{F_A}{\overline{A}}$ [%]	$\frac{F_B}{\overline{B}}$ [%]	$\frac{F_C}{\overline{C}}$ [%]
3301	100	85	7.2	15.4	5.7	230	61	290	3.6	3.9	1.4	7.5	2.4	5.0	3%	4%	2%
3302	150	122	7.2	16.1	7.1	284	54	337	3.6	4.0	1.8	7.6	2.2	5.4	3%	4%	2%
3303	150	123	6.0	15.1	7.1	429	51	480	3.0	3.8	1.8	6.8	2.0	4.8	2%	4%	1%
3304	114	90	5.6	14.4	5.4	271	47	318	2.8	3.6	1.3	6.4	2.3	4.1	2%	5%	1%
Well13	124	105	6.5	19.3	5.7	232	62	294	3.2	4.8	1.4	8.1	3.4	4.7	3%	5%	2%
TEG371up	150	121	6.7	16.3	7.5	210	58	268	3.4	4.1	1.9	7.4	2.2	5.2	4%	4%	2%
TEG371op	37	32	5.1	9.4	4.2	31	59	91	2.6	2.3	1.1	4.9	1.3	3.6	16%	2%	4%
3312	152	121	3.6	4.9	5.0	17	34	52	1.8	1.2	1.2	3.0	0.0	3.0	17%	0%	6%
3313	152	121	9.6	16.0	10.4	55	73	128	4.8	4.0	2.6	8.8	1.4	7.4	16%	2%	6%
TEG372	152	121	6.1	9.6	6.6	31	56	87	3.0	2.4	1.6	5.4	0.8	4.7	18%	1%	5%

Tab. 3: Stochastic properties for the observed head differences. N denotes how often data quality allows determining secondary observations A, B and C. The columns $\overline{A}$, $\overline{B}$, $\overline{C}$ are the mean values of the corresponding secondary observations. The last three columns contain the relative error for the secondary observations A, B, C.

observation well	screen elevation [m asl]	bank distance [m]	oxygen [mg/l]	nitrate [mg/l]	manganese [mg/l]	iron [mg/l]	ammonium [mg/l]	total N [mg/l]
3301	11.9	25	0.4	0.1	0.5	0.2	0.5	0.4
3302	11.2	60	0.4	2	0.3	0.1	0.1	0.6
3303	14.4	85	0.5	0.7	0.3	ND	0.2	0.4
TEG371op	22.7	30	1	2.7	0.3	0.1	0.1	0.7
TEG371up	16.9	30	0.3	ND	0.6	0.7	0.6	0.6
TEG372	23.7	65	2	5	ND	ND	ND	1.1

Tab. 4: Position and geochemical properties of observation wells from transect. The elevation is the center of the screen in m asl, distance is measured perpendicular to the bank. The redox sensitive components are mean concentrations between January 2003 and August 2004, ND denotes the species is below detection limit.